Journal of Applied Electrochemistry **29**: 829–836, 1999.

Mass transfer and current efficiency for the electrodeposition of silver in fluorosilicic acid solution

J.-S. DO* and A.-S. HER
Department of Chemical Engineering, Tunghai University, Taichung, Taiwan, 40704 ROC
*(*author for correspondence)*

Received 24 March 1997; accepted in revised form 4 January 1999

Key words: current efficiency, electrodeposition, fluorosilicic acid, mass transfer, silver

Abstract

The stripping and electrodeposition of silver in fluorosilicic acid solution are irreversible reactions as indicated by cyclic voltammetry. The rate constant for the intrinsic heterogeneous cathodic deposition of silver was obtained as $k_C^0 = 40.77 \exp(1.88 - 29.43\, E_C^{0'})$ and the diffusion coefficient of the silver ion in fluorosilicic acid solution as 5.17×10^{-5} cm^2 s^{-1}. Theoretical calculations of the concentration of silver ion correlated well with experimental data. The relationship between the diffusion layer thickness and the stirring rate was also obtained. Increasing the stirring rate and temperature, and decreasing the current density and concentration of fluorosilicic acid, caused an increase in the current efficiency for silver deposition on graphite.

1. Introduction

Silver powder is an important material used in silver paints, conductive pastes and resins, printed circuit boards and contacts, and also as an electrode in batteries, as well as being a catalyst for a number of chemical reactions [1], for example, the oxidation of methanol to formaldehyde. Three conventional methods are available for producing silver powder. The first is the physical method [2, 3] in which molten silver is injected into a low temperature fluid (gas or liquid) and cooled to a solid silver powder. Another method is the chemical reduction of silver ion and suspended silver peroxide particles in solution [3–8]. Formaldehyde, glycerin, hydrazine and glucose have been used for reducing silver ions to powder form [4–7]. Silver–palladium alloy powder can also be produced by adding hydrazine to an acidic solution containing silver and palladium ions [8].

The third method is the cathodic reduction of silver ions. The electrodeposition method for the production of silver powder has several advantages: (a) the procedure is relatively simple; (b) high purity silver powder is obtained; and (c) the properties of silver powder can be controlled by altering the electrochemical experimental parameters, for example, electrolyte composition, concentration of silver ion in the solution, temperature, agitation rate and current density. Previous literature has described the feasibility of electrodepositing silver in silver nitrate [3, 9–13], silver sulfate [10, 14], fluorosilicic acid [10, 15] and silver cyanide [1] solutions.

Recently, light, small and portable electronic devices have been widely used in a variety of applications, mainly for consumer use. A light weight, small volume, high energy density power source is needed to satisfy the requirements of such applications. The silver–zinc battery has been widely used in military and space applications due to its higher energy density. This battery is a highly promising candidate as a power source for use in portable electronic devices. Silver powder produced in fluorosilicic acid electrolyte has the properties of a small apparent density and light colour, and is appropriate for manufacturing silver electrodes used in silver–zinc batteries [10, 15]. The silver electrodes are porous, of regular structure and produce a flat discharge voltage curve when used in the silver–zinc battery [10]. However, the mass transfer characteristics and the factors affecting the current efficiency of the electrodepostion of silver ion in fluorosilicic acid solution still remain unclear.

This study examines the characteristics of the cathodic deposition of silver on graphite in fluorosilicic acid solution by cyclic voltammetry. The mass transfer

coefficient, diffusivity, the diffusion layer and the factors affecting the current efficiency of the cathodic deposition of silver powder are also discussed.

2. Experimental details

2.1. *Cyclic voltammetry*

Graphite was polished with fine emery paper and washed with distilled water in an ultrasonic cleaner. Cyclic voltammetry was performed in an undivided cell with graphite as working electrode, a platinum wire as counter electrode, and Ag/AgCl/3 M KNO_3 (0.410 V vs NHE) as a reference electrode. An electrochemical analyser (BAS 100B) was used to perform the experiment. All potentials are referred to the Ag/AgCl/3 M KNO_3 electrode.

2.2. *Cathodic deposition of silver powder*

A silver plate of 5 cm × 3 cm × 0.5 cm was used as anode. The silver plate was polished with fine emery paper and washed with distilled water in an ultrasonic cleaner for 15 min. The silver plate was dipped in a 10% HCl aqueous solution for 15 min to remove oxides formed on the surface and then washed with distilled water. The silver plate was then dipped in a 10% NaOH aqueous solution to remove the grease on the surface. Finally, the plate was washed with distilled water again. A graphite plate, pretreated as described in the above section, was used as the cathode for electrodepositing the silver powder. The experiment was performed in a 1000 ml plastic beaker with an axial flow stirrer. Power (d.c.) was supplied with a potentiostat/galvanostat (Nichia G1005E).

3. Results and discussion

3.1. *Cyclic voltammograms*

Figure 1 depicts cyclic voltammograms of 8 mM $AgNO_3$ at various scan rates using 0.1 M H_2SiF_6 and graphite as electrolyte and working electrode. The reduction peaks represent the deposition of silver ion

$$Ag^+ + e^- \rightarrow Ag \tag{1}$$

The anodic peaks denote the anodic oxidation of silver deposited on the graphite to argentic oxide

$$2Ag + H_2O \rightarrow Ag_2O + 2H^+ + 2e^- \tag{2}$$

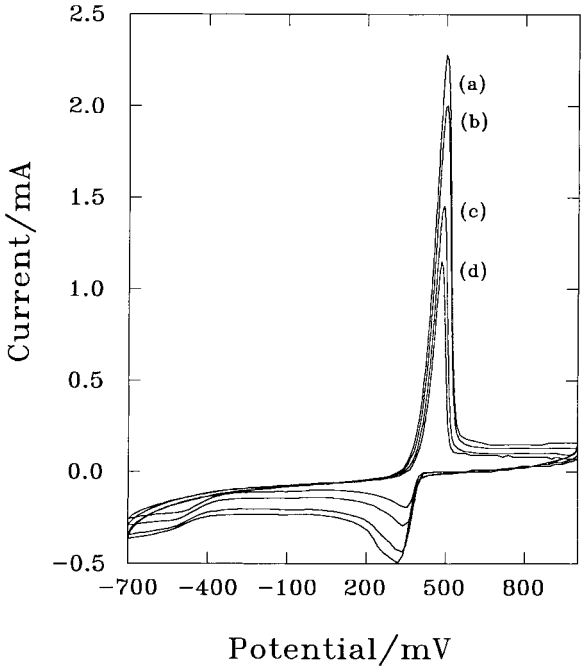

Fig. 1. Cyclic voltammetry of the electrodeposition of silver ion. Working electrode: graphite (area 0.14 cm^2), counter electrode: Pt wire, reference electrode: Ag/AgCl/3M KNO_3, $[Ag^+] = 0.008$ M, electrolyte: 0.1 M H_2SiF_6, $T = 30\,^{\circ}C$. Scanning rate: (a) 60, (b) 40, (c) 20, (d) 10 mV s^{-1}.

The generated argentic oxide is dissolved in the fluorosilicic acid solution

$$Ag_2O + 2H^+ \rightarrow 2Ag^+ + H_2O \tag{3}$$

The anodic and cathodic peak currents increase with increasing scan rate (Figure 1). Increasing the scan rate from 10 to 60 mV s^{-1} causes the reduction peak current to increase from 0.19 to 0.50 mA and the peak potential to decrease from 350 to 319 mV. The straight lines are obtained by plotting the cathodic peak current against the square root of the scan rate ($v^{1/2}$) and the peak potential against logarithmic scan rate (ln v) as shown in Figures 2 and 3.

The cathodically reduced silver ion on the graphite is shown to be a totally irreversible reaction [16]. The relationship [16] between the peak current and the peak potential is

$$\ln i_{pC} = \left[\ln(0.227\, n_C F A C^*_{Ag^+} k^0_C) + \frac{\alpha n_{Cd} F}{RT} E^{0\prime}_C\right] - \frac{\alpha_C n_{Cd} F}{RT} E_{pC} \tag{4}$$

where n_C, F, A, k^0_C, $C^*_{Ag^+}$, α_C, n_{Cd} and $E^{0\prime}_C$ denote the number of electrons per silver ion reduced, faraday

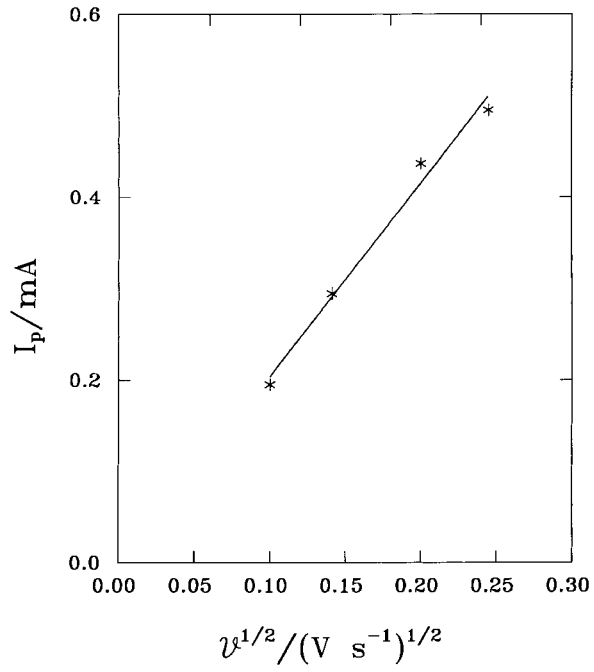

Fig. 2. Plot of I_p against $v^{1/2}$. Working electrode: graphite (area 0.14 cm^2), counter electrode: Pt wire, reference electrode: Ag/AgCl/3 M KNO_3, $[Ag^+] = 0.008$ M, electrolyte: 0.1 M H_2SiF_6 $T = 30$ °C.

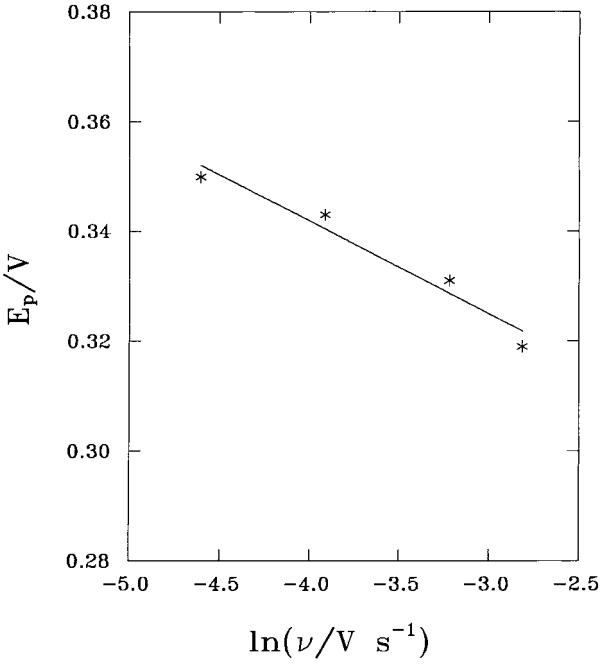

Fig. 3. Plot of E_p against ln v. Working electrode: graphite (area 0.14 cm^2), counter electrode: Pt wire, reference electrode: Ag/AgCl/3 M KNO_3, $[Ag^+] = 0.008$ M, electrolyte: 0.1 M H_2SiF_6, $T = 30$ °C.

constant, surface area of working electrode, intrinsic heterogeneous cathodic reaction rate constant, concentration of silver ion in the bulk solution, cathodic transfer coefficient, number of electrons involved in the cathodic rate determining step, and cathodic formal potential, respectively. A straight line is obtained from plotting the logarithmic peak current against peak potential as in Figure 4. The slope of the straight line is −29.43, corresponding to an $\alpha_C n_{Cd}$ value of 0.76. The intercept of this line is 1.88 and the intrinsic heterogeneous cathodic reaction rate constant is obtained as

$$k_C^0 = 40.77 \exp(1.88 - 29.43 E_C^{0'}) \quad (5)$$

The values of $\alpha_C n_{Cd}$ and k_C^0 are only approximate because the correlation between experimental data and Equation 4 is not completely perfect.

3.2. *Electrodeposition of silver powder*

3.2.1. *Effect of stirring rate*

The concentration of silver ion in the electrolyte is initially zero. The concentration of silver ion increases sharply from 0 to 13.2 mM when the charge increases from 0 to 900 C at a stirring rate of 1000 rpm. The rate of electrodepositing silver (the consumption of silver ion) on the cathode increases because of the increase in silver ions in the solution when the run time increases.

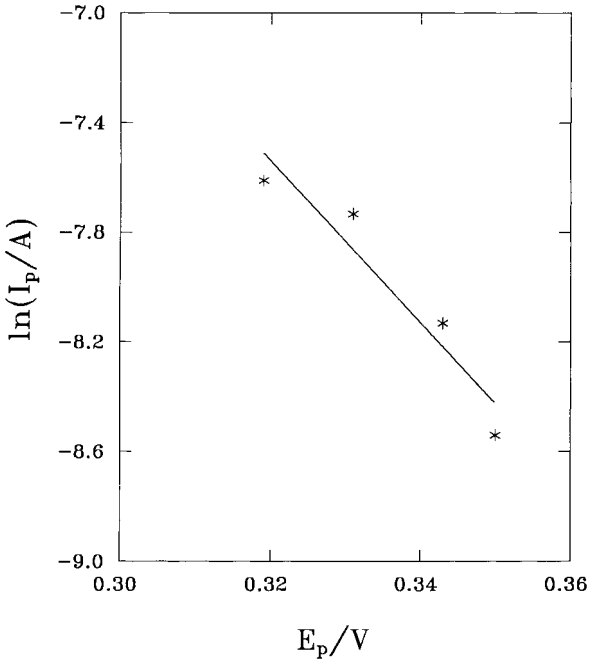

Fig. 4. Plot of ln I_p against E_p. Working electrode: graphite (area 0.14 cm^2), counter electrode: Pt wire, reference electrode: Ag/AgCl/3 M KNO_3, $[Ag^+] = 0.008$ M, electrolyte: 0.1 M H_2SiF_6, $T = 30$ °C.

At the same time, the rate of stripping of silver (the generation of silver ions) from the anode is constant due to the constant current applied. The increase in concentration of silver ion thus slows down as the electrolysis time increases. The generation of silver ions from the anode is then equal to the consumption of silver ions at the cathode. A steady silver ion concentration is ultimately reached. The experimental results demonstrate that the steady state concentration of silver ions is 15.0 mM at a charge exceeding 1800 C and a constant stirring rate of 1000 rpm (Figure 5).

Increasing the stirring rate from 100 to 1000 rpm causes the steady state concentration to decrease from 43.0 to 15.0 mM (Figure 5). When the system reaches steady state, the stripping current is equal to the deposition current and is proportional to the mass transfer rate of silver ion from bulk solution to cathodic surface.

$$i_{\text{stripping}} = i_{\text{deposition}} \propto k_{\text{m}}(C^{\text{b}}_{\text{Ag}^+} - C^{\text{s}}_{\text{Ag}^+}) \tag{6}$$

where k_{m}, $C^{\text{b}}_{\text{Ag}^+}$ and $C^{\text{s}}_{\text{Ag}^+}$ denote the mass transfer coefficient, the concentrations of silver ions in the bulk solution and at the cathodic surface, respectively.

When the reaction is controlled by the mass transfer rate, the concentration of silver ions at the cathodic surface approaches zero. Therefore, the deposition rate is proportional to the product of the mass transfer coefficient and the silver ion concentration in the bulk solution. When the constant current is applied, the generation of silver ions by stripping silver from the anode remains constant for various stirring rates. Increasing the stirring rate causes the diffusion layer thickness to decrease and the mass transfer coefficient (k_{m}) to increase. Since the stripping current is maintained constant, the right hand side of Equation 6 remains constant. As a result, the silver ion concentration decreases as both the stirring rate and mass transfer coefficient increase.

When the stirring rate decreases, the concentration of silver ion increases, which subsequently causes a decrease in the overall current efficiency for cathodic silver powder production. As seen in Figure 6, the overall current efficiency decreases from 88.0 to 66.1% when the stirring rate decreases from 1000 to 100 rpm at a charge of 10800 C.

3.2.2. *Mass transfer of silver ion*

If the current efficiency for stripping silver from anode is assumed to be 100%, the mass balance for the silver ion in the bulk solution is

$$V\frac{\mathrm{d}C^{\text{b}}_{\text{Ag}^+}}{\mathrm{d}t} = \frac{I}{nF} - k_{\text{m}}AC^{\text{b}}_{\text{Ag}^+} \tag{7}$$

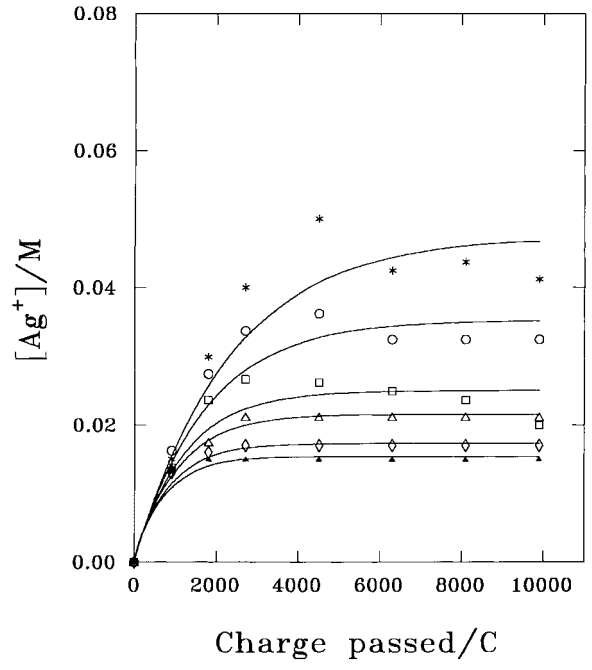

Fig. 5. Effect of charge passed on the concentration of silver ion for various stirring rate. Cathode: graphite (area 77 cm^2); anode: silver plate (area 34 cm^2), $[H_2SiF_6] = 0.208$ M. Volume of solution 500 ml; cathodic current density 39 mA cm^{-2}, $T = 40$ °C. Stirring rate: (⋆) 100, (○) 200, (□) 300, (△) 500, (◇) 800 and (▲) 1000 rpm.

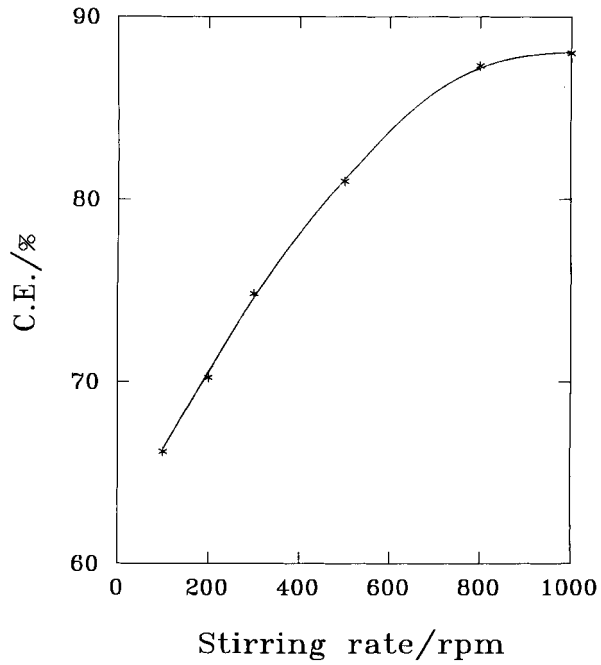

Fig. 6. Effect of stirring rate on the current efficiency. Cathode: graphite (area 77 cm^2); anode: silver plate (area 34 cm^2), $[H_2SiF_6] = 0.208$ M. Volume of solution 500 ml; cathodic current density 39 mA cm^{-2}; $T = 40$ °C, charge passed = 10 800 C.

where V, I and A are the volume of the electrolyte, the applied current and the cathodic surface area, respectively. The first and second terms on the right hand side of Equation 7 represent the generation of silver ion from the anodic stripping of silver and the consumption of silver ion by the cathodic deposition of silver powder, respectively. The first order ordinary differential equation is solved as

$$C^{b}_{Ag^+} = \frac{I}{nFk_mA}\left(1 - \exp\left(-\frac{k_mA}{V}t\right)\right) \quad (8)$$

Figure 5 compares the theoretical calculation of the concentration of silver ion with experimental results. The theoretical calculations basically correlate well with the experimental data. Definite concentration peaks are formed at stirring rates less than 300 rpm before settling down to more steady values (Figure 5). The experimental results show slow nucleation (slow consumption of silver ions) in the initial stage of deposition, resulting in a higher concentration of silver ions than predicted. Increasing the run time causes formation of silver dendrites, which increases the surface area of the cathode. The consumption of silver ions (deposition of silver) hence increases and the concentration of silver ions decreases.

Table 1 lists the mass transfer coefficients (k_m) for various stirring rates. The mass transfer coefficient increases from 0.008 52 to 0.0210 cm s^{-1} with an increase of the stirring rate from 100 to 500 rpm. The mass transfer coefficient can be expressed as

Table 1. Mass transfer coefficients of silver ion in the fluorosilicic acid solution. Cathode: graphite; cathode area 77.0 cm^2; anode: silver plate; anode area 34.0 cm^2; cathodic current density 39 mA cm^{-2}, $[Ag^+]_i$ = 0 M

Stirring rate /rpm	Temp. /°C	$[H_2SiF_6]$ /mM	k_m /cm s^{-1}	Error*
100	40	208	0.00852	1.93×10^{-10}
200	40	208	0.0114	8.45×10^{-11}
300	40	208	0.0161	6.88×10^{-11}
500	40	208	0.0210	5.43×10^{-12}
800	40	208	0.0233	3.45×10^{-12}
1000	40	208	0.0262	7.47×10^{-12}
600	5	208	0.0138	4.93×10^{-11}
600	10	208	0.0157	4.17×10^{-11}
600	20	208	0.0172	3.21×10^{-11}
600	30	208	0.0201	1.94×10^{-11}
600	50	208	0.0242	4.00×10^{-12}
600	65	208	0.0333	3.30×10^{-12}
600	5	69	0.0172	5.44×10^{-12}
600	5	139	0.0159	2.69×10^{-11}
600	5	278	0.0128	6.13×10^{-11}

* error = $\sum_{i=1}^{n}\left([Ag^+]_{exp} - [Ag^+]_{theo}\right)^2$

$$k_m = D_{Ag^+}/L \quad (9)$$

where D_{Ag^+} and L denote the diffusion coefficient of silver ion and the diffusion layer thickness, respectively. In general, the relationship between the diffusion layer thickness and the stirring rate [16, 17] is

$$L = ar^{-b} \quad (10)$$

where r represents the stirring rate, and a and b are constants. Substituting Equation 10 into Equation 9, the relation between mass transfer coefficient and the stirring rate is

$$\ln k_m = \ln\frac{D_{Ag^+}}{a} + b \ln r \quad (11)$$

A straight line is obtained by plotting the log of mass transfer coefficient against log of stirring rate, as illustrated in Figure 7. Notably, the value of b obtained from the slope of the straight line is 0.49. The intercept is −7.0, which corresponds to a value of D_{Ag^+}/a of 9.12×10^{-4} cm $(rpm)^{-0.49}$ s^{-1}.

Because the cathodic deposition of silver ion on graphite is totally irreversible, the relation of the peak current to the scan rate [16] is

$$i_p = (2.99 \times 10^5)n(\alpha n_a)^{1/2}AC^{b}_{Ag^+}D^{1/2}_{Ag^+}v^{1/2} \quad (12)$$

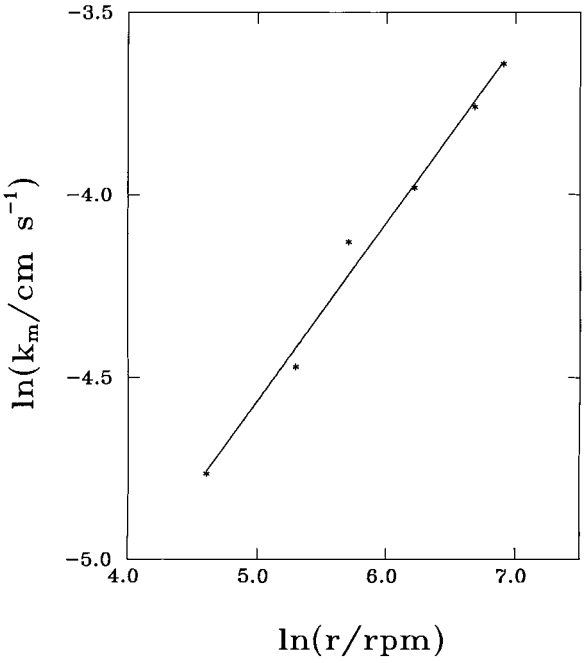

Fig. 7. Plot of ln k_m against ln r. Cathode: graphite (area 77 cm^2); anode: silver plate (area 34 cm^2), $[H_2SiF_6]$ = 0.208 M. Volume of solution 500 ml; cathodic current density 39 mA cm^{-2}, T = 40 °C.

The slope of the straight line obtained from the plot of i_p against $v^{1/2}$ (Figure 2) is 0.0021 $A(V\ s^{-1})^{-1/2}$, as shown in Equation 13

$$(2.99 \times 10^5)n(\alpha n_a)^{1/2}AD_{Ag^+}^{1/2}C_{Ag^+}^{b} = 0.0021 \quad (13)$$

Substituting the relevant parameters into Equation 13 yields a diffusion coefficient for silver ion at 30 °C of 5.17×10^{-5} cm^2 s^{-1}. Both the empirical correlation and the Stokes–Einstein equation indicate that the diffusivity of solute in the liquid phase is first order proportional to the temperature [18, 19]. Correspondingly, the diffusivity of silver ion at 40 °C is estimated as 5.34×10^{-5} cm^2 s^{-1}. Substituting the diffusion coefficient at 40 °C the term D_{Ag^+}/a yields a value for the constant a of 0.059 cm rpm$^{0.49}$. Therefore, the relationship between the diffusion layer thickness and the stirring rate is

$$L = 0.059\,r^{-0.49} \quad (14)$$

3.2.3. *Effect of temperature*

Figure 8 shows that the concentration of silver ions for various temperatures obtained from the experimental data correlates well with the theoretical calculations.

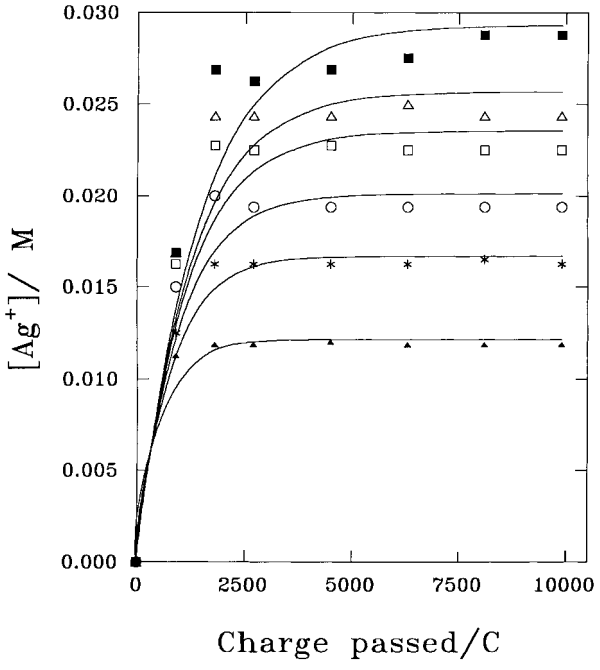

Fig. 8. Effect of charge passed on the concentration of silver ion for various temperature. Cathode: graphite (area 77 cm^2); anode: silver plate (area 34 cm^2), $[H_2SiF_6] = 0.208$ M. Volume of solution 500 ml; cathodic current density 39 mA cm^{-2}; stirring rate 600 rpm. Temperature: (■) 5, (△) 10, (□) 20, (○) 30, (⋆) 50 and (▲) 65 °C.

Increasing the temperature from 5 to 65 °C causes an increase of the mass transfer coefficient for the silver ion from 0.0138 to 0.0333 cm s^{-1} at a stirring rate of 600 rpm (Table 1). On the one hand, the solution viscosity and the diffusion layer thickness decrease as temperature increases. On the other hand, the diffusivity of silver ion increases with temperature [18, 19]. According to Equation 9, the mass transfer coefficient increases with temperature. Interestingly, Equation 6 shows that maintaining the current constant and increasing the temperature results in a decrease in concentration of silver ions and an increase in current efficiency for silver powder deposition. Experimental results indicate that the steady state concentration of silver ions decreases from 29.0 to 12.0 mM with an increase in temperature from 5 to 65 °C (Figure 8). Moreover, accompanying this temperature increase from 5 to 65 °C with a decrease in silver ion concentration increases the current efficiency from 87.0 to 93.0%.

3.2.4. *Effect of current density*

Increasing the applied current density increases both the generation of silver ions and the consumption of silver ions at steady state. Notably, the mass transfer coefficient stays fixed if the temperature and the stirring rate remain constant. Increasing the applied current density increases the concentration of silver ions which decreases the current efficiency for silver powder production. The steady state concentration of silver ions increases from 15.0 to 54.0 mM when the current density increases from 39 to 258 mA cm^{-2}, respectively. Moreover, increasing current density may cause a side reaction (i.e., the evolution of hydrogen) on the cathode. This would decrease the current efficiency for silver powder deposition. According to Figure 9, increasing the current density from 39 to 258 mA cm^{-2} leads to a decrease from 90.0 to 71.0% in current efficiency.

3.2.5. *Effect of concentration of fluorosilicic acid*

The physical properties of the electrolyte, such as viscosity, change with varying fluorosilicic acid concentration. The steady concentration of silver ions increases from 23.1 to 30.0 mM when the concentration of fluorosilicic acid is increased from 69 to 278 mM, as illustrated in Figure 10. The mass transfer coefficient decreases from 0.0172 to 0.0128 cm s^{-1} with increase in fluorosilicic acid concentration from 69 to 278 mM (Table 1). An increase in fluorosilicic acid concentration increases the viscosity of the electrolyte, which leads to a decrease in the mass transfer coefficient, and an increase in the concentration of silver ions. In addition, the increasing concentration of silver ions causes a decrease in the current efficiency for silver powder deposition.

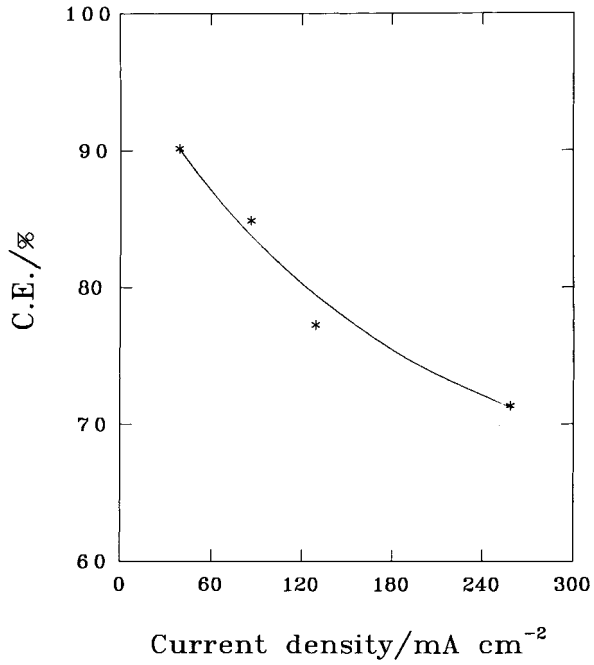

Fig. 9. Effect of current density on the current efficiency. Cathode: graphite (area 23 cm^2); anode: silver plate (area 10 cm^2), $[H_2SiF_6]$ = 0.139 M. Volume of solution 150 ml; stirring rate 600 rpm; $T = 5$ °C; charge passed 3240 C.

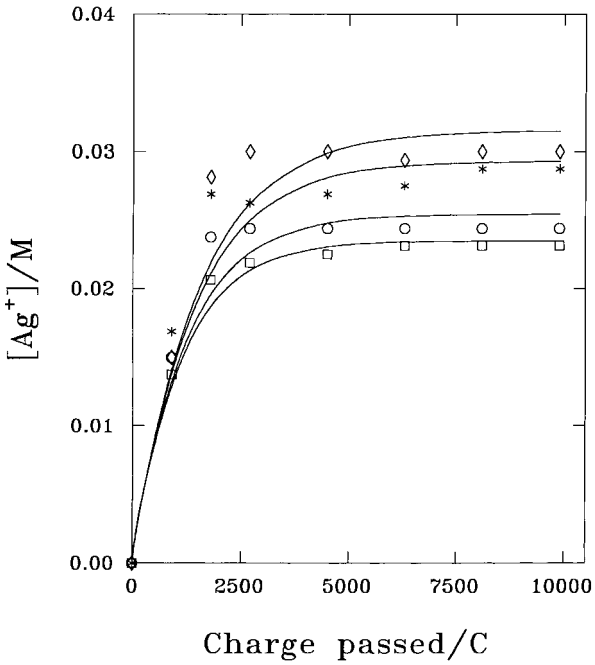

Fig. 10. Effect of charge passed on the concentration of silver ion for various concentration of fluorosilicic acid. Cathode: graphite (area 77 cm^2); anode: silver plate (area 34 cm^2). Volume of solution 500 ml; cathodic current density 39 mA cm^{-2}; $T = 5$ °C; stirring rate 600 rpm. $[H_2SiF_6]$: (□) 69, (○) 139, (⋆) 208 and (◇) 278 mM.

Increasing the concentration of fluorosilicic acid from 69 to 278 mM is shown to decrease the current efficiency from 87.0 to 85.0%.

4. Conclusions

Cyclic voltammetry performed demonstrates that the cathodic deposition of silver ions on graphite is a totally irreversible reaction. The cathodic peak current increases from 0.19 to 0.50 mA and the peak potential decreases from 350 to 319 mV as the scan rate increases from 10 to 60 mV s^{-1}. The intrinsic heterogeneous reaction rate constant and the value of $\alpha_C n_{Cd}$ are approximately obtained as $40.77 \exp(1.88 - 29.43 E_c^{0'})$ and 0.76. The diffusion coefficient of silver ion is evaluated as 5.17×10^{-5} cm^2 s^{-1} at 40 °C in 208 mM H_2SiF_6 aqueous solution. Theoretical calculations of the concentration of silver ions correlate well with experimental data. Increasing the stirring rate and the temperature while decreasing the concentration of fluorosilicic acid has three interrelated effects. First, it increases the mass transfer coefficient, which in turn, decreases the concentration of silver ions. This latter effect leads to an increase in the current efficiency for silver powder deposition.

Acknowledgement

The authors would like to thank the National Science Council of the Republic of China (NSC 84-2214-E-029-004), Chung Shan Institute of Science and Technology and Tunghai University for support.

References

1. A.T. Kuhn, P. Neufeld and G. Butler, *Surf. Technol.* **16** (1982) 1.
2. Y. Kito, T. Sakuta, T. Mizuno and T. Morita, *J. Powder Metal* **25** (1989) 13.
3. F. Montino and L. Colombo, *US Patent 4 039 317*. (1977).
4. O.A. Short and N.J. Metochen, *US Patent 2 752 237*. (1956).
5. J.Y. Wu, *Producing Fine Silver Powder*, MS thesis of National Central University, Chung Li, Taiwan, ROC (1993).
6. E.M. Jost and P. Mass, *US Patent 4 456 473*. (1984).
7. E.M. Jost and P. Mass, *US Patent 4 456 474*. (1984).
8. T. Hayashi, *European Patent 0 249 366*. (1987).
9. M.G. Pavlovic, M.D. Maksimovic and K.I. Popov, *J. Appl. Electrochem.* **8** (1978) 61.
10. A. Calusaru, *Electrodepostion of Metal Powder*, Elsevier Scientific, New York (1979) pp. 345–7.
11. J.Y. Lee and T.C. Tan, *J. Electrochem. Soc.* **137** (1990) 1402.
12. K.I. Popov, B.A. Mitrovic, M.G. Pavlovic and B.V. Toperic, *J. Appl. Electrochem.* **21** (1991) 50.
13. E. Michailova and A. Milchev, *J. Appl. Electrochem.* **21** (1991) 170.

14. M.E. Martins, R.C. Salvarezza, J.M. Vara and A.J. Arvia, *J. Electrochem. Soc.* **138** (1991) 2509.
15. K.N. Brown and N.J. Teaneck, *US Patent 2 810 682*. (1957).
16. A.J. Bard and L.R. Faulkner, *Electrochemical Methods: Fundamentals and Applications*, J. Wiley & Sons, New York, (1980).
17. T.C. Chou, J.S. Do, B.J. Hwang and J.J. Jow, *Chem. Eng. Comm.* **51** (1987) 47.
18. R.B. Bird, W.E. Stewart and E.N. Lightfoot, *Transport Phenomena*, J. Wiley & Sons, New York, (1960) p. 514.
19. R.H. Perry and C.H. Chilton, *Chemical Engineer's Handbook*, 5th edn, McGraw-Hill, New York (1973) pp. 3–234.